

# The Murine Gammaherpesvirus 68 M2 Gene Is Required for Efficient Reactivation from Latently Infected B Cells

Jeremy Herskowitz, Meagan A. Jacoby, and Samuel H. Speck\*

*Center for Emerging Infectious Diseases, Yerkes National Primate Research Center, School of Medicine, Emory University, Atlanta, Georgia*

Received 22 July 2004/Accepted 1 October 2004

**Murine gammaherpesvirus 68 ( $\gamma$ HV68) infection of mice provides a tractable small-animal model system for assessing the requirements for the establishment and maintenance of gammaherpesvirus latency within the lymphoid compartment. The M2 gene product of  $\gamma$ HV68 is a latency-associated antigen with no discernible homology to any known proteins. Here we focus on the requirement for the M2 gene in splenic B-cell latency. Our analyses showed the following. (i) Low-dose (100 PFU) inoculation administered via the intranasal route resulted in a failure to establish splenic B-cell latency at day 16 postinfection. (ii) Increasing the inoculation dose to  $4 \times 10^5$  PFU administered via the intranasal route partially restored the establishment of B-cell latency at day 16, but no virus reactivation was detected upon explant into tissue cultures. (iii) Although previous data failed to detect a phenotype of the M2 mutant upon high-dose intraperitoneal inoculation, decreasing the inoculation dose to 100 PFU administered intraperitoneally revealed a splenic B-cell latency phenotype at day 16 that was very similar to the phenotype observed upon high-dose intranasal inoculation. (iv) After low-dose intraperitoneal inoculation, fractionated B-cell populations showed that the M2 mutant virus was able to establish latency in surface immunoglobulin D-negative (sIgD<sup>-</sup>) B cells; by 6 months postinfection, equivalent frequencies of M2 mutant and marker rescue viral genome-positive sIgD<sup>-</sup> B cells were detected. (v) Like the marker rescue virus, the M2 mutant virus also established latency in splenic naive B cells upon low-dose intraperitoneal inoculation, but there was a significant lag in the decay of this latently infected reservoir compared to that seen with the marker rescue virus. (vi) After low-dose intranasal inoculation, by day 42 postinfection, latency was observed in the spleen, although at a frequency significantly lower than that in the marker rescue virus-infected mice; by 3 months postinfection, nearly equivalent levels of viral genome-positive cells were observed in the spleens of marker rescue virus- and M2 mutant virus-infected mice, and these cells were exclusively sIgD<sup>-</sup> B cells. Taken together, these data convincingly demonstrate a role for the M2 gene product in reactivation from splenic B cells and also suggest that disruption of the M2 gene leads to dose- and route-specific defects in the efficient establishment of splenic B-cell latency.**

Gammaherpesviruses are lymphotropic viruses that are capable of establishing a lifelong infection of the host. These viruses infect a diverse variety of mammalian species and are associated with the development of malignancies and lymphoproliferative diseases. Studies of the pathogenesis of the human gammaherpesviruses Epstein-Barr virus (EBV) and Kaposi's sarcoma-associated herpesvirus have been hampered by a restricted host range and thus have been confined largely to *in vitro* analyses. Murine gammaherpesvirus 68 ( $\gamma$ HV68) is a type 2 gammaherpesvirus and shares genome colinearity with EBV and Kaposi's sarcoma-associated herpesvirus (5, 6, 32, 37).  $\gamma$ HV68 infection of mice represents an established, genetically tractable small-animal model system with which to study gammaherpesvirus pathogenesis, host control, and tumor induction (3, 4, 14, 15, 20, 21, 31).

$\gamma$ HV68 is a natural pathogen of wild murid rodents and is capable of infecting both inbred and outbred mice (1, 13, 19, 24). Upon inoculation of inbred strains of mice,  $\gamma$ HV68 undergoes acute-phase replication in multiple organs, including the lungs and spleen. Subsequently, a latent infection is established; this infection is marked by CD4<sup>+</sup>-T-cell-dependent

splenomegaly, which peaks at 14 to 21 days postinfection (dpi) (7, 22, 24, 25, 29, 34). As in EBV infection, B lymphocytes appear to harbor the majority of  $\gamma$ HV68 latency (8, 25, 37). However, macrophages (8, 36), dendritic cells (8), and lung epithelial cells (23) have also been implicated as sites of  $\gamma$ HV68 latency.

Recently, it was shown that at early times postinfection,  $\gamma$ HV68, like EBV, resides within various B-cell populations, while long-term latency is predominantly confined to memory B cells (isotype-switched mature B cells lacking surface immunoglobulin D [sIgD]) (26, 27). Access to the memory B-cell compartment allows EBV and  $\gamma$ HV68 to maintain long-term latency within a long-lived, immunologically privileged site in the host. At present, there is growing evidence to support the notion that EBV is capable of usurping the natural B-cell differentiation pathway in order to access the memory B-cell reservoir. It has been hypothesized that upon infection of naive B cells, a subset of EBV genes are expressed and subsequently provide the necessary signals to drive the infected B cells to proliferate. Once activated, these infected B cells participate in germinal center reactions, in which specific EBV latency-associated gene products are capable of providing the requisite signals to exit the cell cycle by differentiating into memory B cells. Once latency is established in the memory compartment, EBV downregulates viral gene expression and utilizes these

\* Corresponding author. Mailing address: Yerkes National Primate Research Center, 954 Gatewood Rd., N.E., Atlanta, GA 30329. Phone: (404) 727-7665. Fax: (404) 727-7768. E-mail: sspeck@rmy.emory.edu.

cells to leave the site of initial infection and traffic to secondary lymphoid organs, including the spleen. Analyses of the impact of specific candidate  $\gamma$ HV68 latency-associated genes on the establishment of long-term latency in memory B cells may identify specific  $\gamma$ HV68 genes necessary for driving B-cell differentiation.

The  $\gamma$ HV68 M2 open reading frame (ORF) is a latency-associated gene located in the unique region at the left end of the viral genome. M2 transcripts have been detected in latently infected splenocytes *in vivo* (10, 33) as well as in murine B-cell lymphoma line S11, which is latently infected with  $\gamma$ HV68 (10). The contributions of M2 to  $\gamma$ HV68 acute-phase replication and latent infection were previously analyzed through the use of viral recombinants containing targeted mutations in the M2 ORF (11, 12). After intranasal inoculation with  $4 \times 10^5$  PFU, the M2 mutant viruses displayed no defect in acute-phase replication in the lungs. However, M2 was shown to be critical for the establishment of latency and reactivation from latency in the spleen at 16 dpi. Surprisingly, M2 was not required for the establishment of latency or for reactivation from latency in the spleen at 16 dpi after intraperitoneal inoculation with  $10^6$  PFU of virus (11). Similarly, in  $\gamma$ HV68 infection of B-cell-deficient mice, splenic latency was established after intraperitoneal inoculation but was not efficiently established after intranasal inoculation (30, 35). However, adoptive transfer of uninfected T-cell-depleted splenocytes could restore  $\gamma$ HV68 splenic latency after intranasal inoculation (23). These analyses suggest that, similar to the way in which EBV utilizes memory B cells to infect secondary lymphoid organs,  $\gamma$ HV68 infection of the spleen after intranasal inoculation may require trafficking of the virus through the infection and/or the establishment of latency in B cells. The present study characterizes the contribution of M2 to the establishment of  $\gamma$ HV68 B-cell latency in the spleen as well as reactivation from latency.

#### MATERIALS AND METHODS

**Viruses and tissue cultures.**  $\gamma$ HV68 WUMS (ATCC VR1465) was the wild-type (wt) virus used to derive the mutants in this study. Virus passage and determination of titers were performed as previously described (2). NIH 3T12 cells and mouse embryonic fibroblasts (MEFs) were maintained in Dulbecco's modified Eagle's medium supplemented with 100 U of penicillin per ml, 100 mg of streptomycin per ml, 10% fetal calf serum (FCS), and 2 mM L-glutamate (cMEM). Cells were maintained at 37°C in a 5% CO<sub>2</sub> environment. MEFs were obtained as previously described (18).

**Generation of virus mutants.** All recombinant viruses were generated by homologous recombination following calcium phosphate or Superfect (Qiagen, Hilden, Germany) cotransfection of  $\gamma$ HV68 genomic DNA and a gene-targeting plasmid as previously described (2, 11). Briefly, a  $\gamma$ HV68 genomic fragment containing the region from bp 2403 to bp 6262 (WUMS sequence) (32) was cloned into the Litmus-38 plasmid (Lit38-M2). The  $\gamma$ HV68M2.Stop targeting construct was created by inserting a 26-bp linker at bp 4314 in Lit38-M2, introducing a translational stop codon after residue 108 of the M2 ORF. The  $\gamma$ HV68M2.Stop virus was generated by Superfect cotransfection of the  $\gamma$ HV68M2.Stop targeting construct and  $\gamma$ HV68M2.LacZ viral DNA (11). The M2 marker rescue virus ( $\gamma$ HV68M2.MR virus) was generated by Superfect cotransfection of  $\gamma$ HV68M2.LacZ viral DNA and Lit38-M2. Both  $\gamma$ HV68M2.Stop and  $\gamma$ HV68M2.MR viruses were isolated after three rounds of plaque purification. Stocks of mutant viruses were generated as previously described (2, 11).

**Mice, infections, and organ harvests.** Female C57BL/6J mice (catalog no. 000664; Jackson Laboratory, Bar Harbor, Maine) were housed at the Yerkes vivarium in accordance with federal and university guidelines. Mice between 8 and 12 weeks of age were placed under isoflurane anesthesia prior to intranasal inoculation with 100 PFU or  $4 \times 10^5$  PFU of virus in 20  $\mu$ l of cMEM or intraperitoneal inoculation with 100 PFU of virus in 0.5 ml of cMEM. Spleens

were harvested into cMEM, homogenized, and filtered through a 100- $\mu$ m-pore-size nylon cell strainer (Becton Dickinson, Franklin Lakes, N.J.). Erythrocytes were removed with red blood cell lysis buffer (Sigma, St. Louis, Mo.). Pooled splenocytes from 5 to 15 mice were used in all experiments.

**Plaque assays.** Plaque assays were performed as previously described (2), with the following modifications. NIH 3T12 cells were plated on six-well plates 1 day prior to infection at  $3 \times 10^5$  cells per well. Organs were subjected to three rounds of mechanical disruption of 1 min each with 1.0-mm zirconium-silica beads (Biospec Products, Bartsville, Okla.) in a Mini-Beadbeater-8 (Biospec Products). Serial 10-fold dilutions of organ homogenates in 200- $\mu$ l volumes were plated on NIH 3T12 cell monolayers. Infection was allowed to proceed for 1 h at 37°C. Immediately after infection and at 3 dpi, plates were overlaid with medium containing Noble agar. At 6 dpi, plates were stained with a Noble agar-neutral red overlay, and plaques were scored on day 7. Titers of all samples were determined in parallel with a known laboratory standard titer. The limit of detection for these assays is 50 PFU per organ.

**Antibodies for flow cytometry.** Cells were stained for fluorescence-activated cell sorting (FACS) with combinations of the following antibodies: phycoerythrin (PE)-conjugated antibodies to CD19 and fluorescein isothiocyanate (FITC)-conjugated antibodies to B220, immunoglobulin D (IgD), IgG1, IgG2a, IgG2b, IgG3, IgA, and IgE. When necessary, rat anti-mouse CD16/CD32 (Fc block) was used to block Fc receptors prior to staining. All reagents were obtained from BD Biosciences Pharmingen, San Diego, Calif.

**Magnetic cell separation.** Murine B cells were isolated by depletion of non-B cells by using a B-cell isolation kit (Miltenyi Biotec, Cologne, Germany). Cells were resuspended at  $2 \times 10^8$ /ml in phosphate-buffered saline (PBS) containing 0.5% FCS, followed by staining with Fc block (0.125  $\mu$ g/10<sup>6</sup> cells) on ice for 15 min. Cells were labeled with PE conjugates at 0.05  $\mu$ g/10<sup>6</sup> cells, FITC conjugates at 0.25  $\mu$ g/10<sup>6</sup> cells, and biotin-antibody cocktail (biotin-conjugated antibodies against CD43, CD4, and Ter-119; mouse B-cell isolation kit from Miltenyi Biotec) for 15 min on ice in the dark, followed by staining with antibiotin Microbeads (Miltenyi Biotec) for 15 min on ice in the dark. Cells were washed twice with PBS containing 0.5% FCS and subjected to magnetic separation by using an autoMACS (Miltenyi Biotec). Following separation, stained cell populations were collected as described below.

**Flow cytometry.** Cells were resuspended at  $5 \times 10^7$ /ml and incubated for 30 min on ice in FACS blocking buffer (8% FCS, 10% normal rabbit serum, 10% normal goat serum, 5% bovine serum albumin, and 0.5 mg of mouse immunoglobulin per ml in Hanks balanced salt solution [0.15 M NaCl, 0.015 M sodium citrate]) or PBS containing 1% FCS and/or an Fc-blocking agent. Cells were stained with PE conjugates at 0.05  $\mu$ g/10<sup>6</sup> cells and FITC conjugates at 0.25  $\mu$ g/10<sup>6</sup> cells by incubation for 1 h on ice in the dark. Cells were washed twice with PBS containing 1% FCS and resuspended at  $5 \times 10^7$ /ml. Stained cell populations were acquired by using a FACSVantage SE (Becton Dickinson, Mountain View, Calif.) flow cytometer. Sorted and unsorted cell populations were resuspended in cMEM supplemented with 10% dimethyl sulfoxide and stored at -80°C for limiting-dilution PCR analyses or resuspended in cMEM at 4°C.

**Limiting-dilution *ex vivo* reactivation analyses.** Limiting-dilution analyses to determine the frequency of cells containing virus capable of reactivation from latency were performed as previously described (34, 36). Briefly, bulk splenocytes or sorted cell populations were resuspended in cMEM and plated in serial twofold dilutions (starting with 10<sup>5</sup> cells) on MEF monolayers in 96-well tissue culture plates. Twelve dilutions were plated per sample, and 24 wells were plated per dilution. Wells were scored for cytopathic effects (CPE) 21 to 28 days postplating. To detect preformed infectious virus, parallel samples of mechanically disrupted cells were plated on MEF monolayers. This process kills >99% of live cells, allowing preformed infectious virus to be discerned from virus reactivated from latently infected cells (34–36). The level of sensitivity of this assay is 0.2 PFU (34).

**Limiting-dilution nested PCR detection of  $\gamma$ HV68 genome-positive cells.** Limiting-dilution analyses to determine the frequency of cells harboring the viral genome were performed by using a single-copy-sensitive nested PCR assay as previously described (35, 36). Briefly, frozen samples were thawed, counted, resuspended in isotonic buffer, and plated in serial threefold dilutions in a background of 10<sup>4</sup> uninfected NIH 3T12 cells in 96-well plates (MWG Biotech, High Point, N.C.). Plates were covered with PCR foil (Eppendorf Scientific, Westbury, N.Y.). Cells were lysed with proteinase K for 6 h at 56°C. Ten microliters of round 1 PCR mixture was added to each well by foil puncture. Following first-round PCR, 10  $\mu$ l of round 2 PCR mixture was added to each well by foil puncture, and samples were subjected to round 2 PCR. All cell lysis and PCR procedures were performed with a PrimusHT thermal cycler (MWG Biotech). Products were resolved by ethidium bromide staining on 2% agarose gels. Twelve PCRs were performed for each sample dilution, and 6 dilutions were used per

sample. Every PCR plate contained control reactions (uninfected cells and 10 copies, 1 copy, and 0.1 copy of plasmid DNA in a background of  $10^4$  cells) as previously described (35, 36). All of the assays demonstrated approximately single-copy sensitivity, with no false-positive results.

**Recovery of  $\gamma$ HV68M2.Stop and  $\gamma$ HV68M2.MR viruses from splenocytes at late times postinfection.** M2 mutant and M2 marker rescue viruses were recovered from splenocytes at 90 dpi by using a recently developed stimulation protocol (13a). Briefly, MEF cells were plated in six-well plates at  $3 \times 10^5$  cells per well 1 day prior to splenocyte harvest. Total splenocytes were resuspended in cMEM containing goat anti-mouse IgM or IgG F(ab')<sub>2</sub> fragment (Jackson ImmunoResearch, West Grove, Pa.) at 10  $\mu$ g/ml and anti-mouse CD40 (BD Biosciences Pharmingen) at 5  $\mu$ g/ml (13a) and plated on MEF monolayers at  $6 \times 10^6$  splenocytes per well. CPEs were observed in wells at 14 days postplating. The contents of wells exhibiting viral CPEs were homogenized, clarified, and divided into aliquots for storage at  $-80^\circ\text{C}$  without further *in vitro* passage. Titers of viral stocks were determined by averaging the values obtained from three independent plaque assays as previously described (2, 11).

**Statistical analyses.** All data were analyzed by using GraphPad Prism software (GraphPad Software, San Diego, Calif.). Data were subjected to nonlinear regression analysis to determine the single-cell frequency for each limiting-dilution analysis. Based on the Poisson distribution, the frequencies of reactivation and viral genome-positive cells were obtained from the nonlinear regression fit of the data, where the regression line intersected at 63.2%.

## RESULTS

**M2 is not required for acute-phase virus replication *in vivo* following low-dose intranasal inoculation.** Previous studies showed that the M2 gene is not required for acute-phase virus replication at various times postinfection (4 and 6 dpi) following intranasal inoculation with  $4 \times 10^5$  PFU in the lungs, where the peak of acute-phase virus replication occurs at 7 dpi (11, 28). Recently, it was shown that the intranasal administration of a lower dose of wt  $\gamma$ HV68 (40 PFU) delays the peak of acute-phase virus replication in the lungs until 10 dpi (28). To assess the role of M2 in latency, it was necessary to determine whether an acute-phase replication defect existed at a lower dose of infection. C57BL/6J mice were infected intranasally with 100 PFU, and viral titers in the lungs were quantified by plaque assays at 6 and 9 dpi. Following intranasal inoculation,  $\gamma$ HV68M2.Stop and  $\gamma$ HV68M2.MR virus titers were comparable at 6 and 9 dpi (Fig. 1). These findings are consistent with previous studies indicating that M2 is not necessary for acute-phase virus replication in the lungs following intranasal inoculation (11, 12).

**M2 is required for the establishment of  $\gamma$ HV68 latency in the spleen following low-dose intranasal inoculation.** Recent experiments by Tibbetts et al. showed that wt  $\gamma$ HV68 latency in the spleen 16 days after intranasal inoculation is independent of the dose of infection (28). Previously, it was shown that the M2 gene is important but not absolutely required for both the establishment of  $\gamma$ HV68 latency and reactivation from latency in bulk splenocytes at 16 dpi following intranasal inoculation with  $4 \times 10^5$  PFU (11). These analyses demonstrated that the  $\gamma$ HV68M2.Stop mutant is capable of establishing latency at a frequency of ca. 1 in 1,000 splenocytes upon intranasal inoculation with  $4 \times 10^5$  PFU, a frequency of latency which is ca. 10-fold lower than the frequency of latency observed in wt virus-infected mice at 16 dpi following intranasal inoculation with  $4 \times 10^5$  PFU (11).

We hypothesized that non-B-cell subsets in the spleen contribute to the latency detected in bulk splenocytes upon infection with an M2 mutant virus. In addition, we were concerned that inoculating mice with high doses of virus might mask a

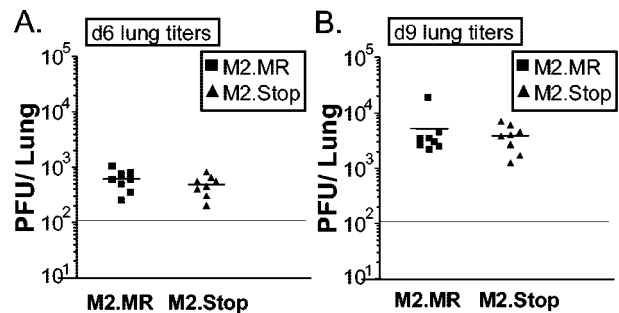


FIG. 1. M2 is not required for acute-phase replication *in vivo* following intranasal inoculation with 100 PFU. (A) C57BL/6 mice were infected intranasally with 100 PFU of either  $\gamma$ HV68M2.Stop or  $\gamma$ HV68M2.MR, and the left lung was extracted at 6 dpi (d6). The results shown were compiled from two independent experiments with three to five mice each. (B) C57BL/6 mice were infected intranasally with 100 PFU of either  $\gamma$ HV68M2.Stop or  $\gamma$ HV68M2.MR, and the left lung was extracted at 9 dpi (d9). The results shown were compiled from two independent experiments with three to five mice each. Virus titers in lungs were determined by plaque assays on NIH 3T12 monolayers. Each point represents the virus titer from a single mouse. The continuous horizontal line indicates the level of detection of the plaque assay (50 PFU), and the short horizontal lines indicate the mean virus titers for the groups.

phenotype of the M2 mutant virus through infection of reservoirs not normally infected at physiologically relevant inocula of virus. Thus, the requirement for M2 during latency in bulk splenocytes and B cells in the spleen was examined following low-dose (100 PFU) intranasal inoculation. Single-cell preparations were generated from spleens harvested from mice infected with wt  $\gamma$ HV68,  $\gamma$ HV68M2.MR, or  $\gamma$ HV68M2.Stop at 16 dpi. Splenocytes were stained with antibodies directed against the pan-B-cell marker CD19 and B220 (Fig. 2), and splenic B cells ( $\text{CD19}^+ \text{B220}^+$ ) were purified by FACS (Fig. 2). To investigate the ability of the M2 mutant virus to be reactivated from latency, splenic B cells and total splenocytes were subjected to a limiting-dilution *ex vivo* reactivation assay (see Materials and Methods) (34, 36). To confirm that the observed virus-induced CPEs were due to reactivated virus and not preformed infectious virus, mechanically disrupted cells were plated in parallel. Importantly, no preformed infectious virus was detected in any experiment in this study (data not shown).

At 16 dpi following intranasal inoculation with 100 PFU, little or no *ex vivo* virus reactivation was observed from either total splenocytes or splenic B cells recovered from mice infected with the M2 mutant virus (Fig. 3). The frequencies of wt  $\gamma$ HV68 and  $\gamma$ HV68M2.MR reactivation from latency in the spleen were 1 in 8,800 and 1 in 9,200 from purified B cells, respectively, and 1 in 8,072 and 1 in 10,400 from unsorted splenocytes, respectively (Fig. 3 and Table 1). In contrast, the frequencies of  $\gamma$ HV68M2.Stop reactivation from latency in splenic B cells and total splenocytes were too low to be accurately determined (Fig. 3A and B). The absence of detectable M2 mutant virus reactivation from latency in B cells and total splenocytes in the spleen could be due to a decrease in the efficiency of reactivation, a decrease in the establishment of latency (measured by the frequency of latently infected cells), or a combination of both.

To assess the requirement for M2 in the establishment of



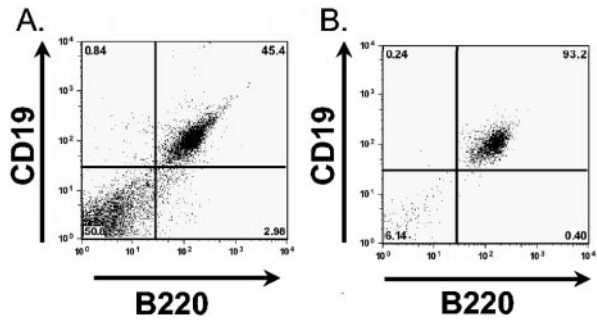


FIG. 2. FACS analysis of purified splenic B lymphocytes. Splenocytes harvested from C57BL/6 mice were prepared as described in Materials and Methods. Splenic B cells were isolated by staining with a PE-conjugated antibody to the pan-B-cell marker CD19 (CD19-PE) and an FITC-conjugated antibody to B220 (B220-FITC). Flow cytometric dot plots from one representative experiment are shown. (A) Presort unfractionated bulk splenocytes stained with CD19-PE and B220-FITC. The CD19<sup>+</sup> B220<sup>+</sup> population represented ca. 40.66%  $\pm$  10.03% (mean  $\pm$  standard error of the mean), 49.45%  $\pm$  4.47%, or 42.26%  $\pm$  11.58% of the total splenocyte population for wt  $\gamma$ HV68,  $\gamma$ HV68M2.Stop, or  $\gamma$ HV68M2.MR infection, respectively, regardless of route or dose of infection and dpi. (B) Postsort FACS analysis indicating the purity of fractionated splenic B lymphocytes. The purity for CD19<sup>+</sup> B220<sup>+</sup> over 11 replicate experiments was 93.9%  $\pm$  0.76%. The extent of contamination of the sorted population was limited to 5.60%  $\pm$  1.85% from the CD19<sup>-</sup> B220<sup>-</sup> fraction.

latency in splenic B cells and unsorted splenocytes, the frequencies of viral genome-positive cells were determined by using a previously described limiting-dilution PCR assay (see Materials and Methods) (35, 36). Splenic B cells and total splenocytes harvested from mice infected with  $\gamma$ HV68M2.Stop harbored nearly undetectable levels of virus (Fig. 3C and D). However, the frequencies of viral genome-positive B cells in the spleen were 1 in 820 for wt  $\gamma$ HV68 and 1 in 580 for  $\gamma$ HV68M2.MR. In unsorted splenocytes, the frequencies of viral genome-positive cells were 1 in 406 for wt  $\gamma$ HV68 and 1 in 600 for  $\gamma$ HV68M2.MR (Fig. 3 and Table 2). These results indicate that the ability of  $\gamma$ HV68 to establish latency in the spleen at 16 dpi is severely compromised in the absence of a functional M2 gene following intranasal inoculation with 100 PFU.

**M2 is required for  $\gamma$ HV68 reactivation from latency in splenic B cells following high-dose intranasal inoculation.** With respect to the M2 phenotype discussed above, previous analyses by Jacoby et al. (11) showed that intranasal inoculation with a higher dose of  $\gamma$ HV68M2.Stop facilitates the establishment of latency in the spleen. As the complete lack of detectable splenic latency following low-dose intranasal inoculation with the M2 mutant virus precluded investigation into potential defects in the establishment of latency in B cells, the ability of  $\gamma$ HV68M2.Stop to establish latency in splenic B cells was examined at a higher dose of infection.

Mice were infected intranasally with  $4 \times 10^5$  PFU of wt  $\gamma$ HV68,  $\gamma$ HV68M2.MR, or  $\gamma$ HV68M2.Stop. At 16 dpi, 1 in 467 splenic B cells (CD19<sup>+</sup> B220<sup>+</sup>) and 1 in 305 bulk splenocytes harbored the viral genome from mice infected with wt  $\gamma$ HV68, as measured by a limiting-dilution PCR assay (Fig. 4C and D). Similar frequencies were found after infection with  $\gamma$ HV68M2.MR (Fig. 4C and D). In contrast, only 1 in 2,100 B

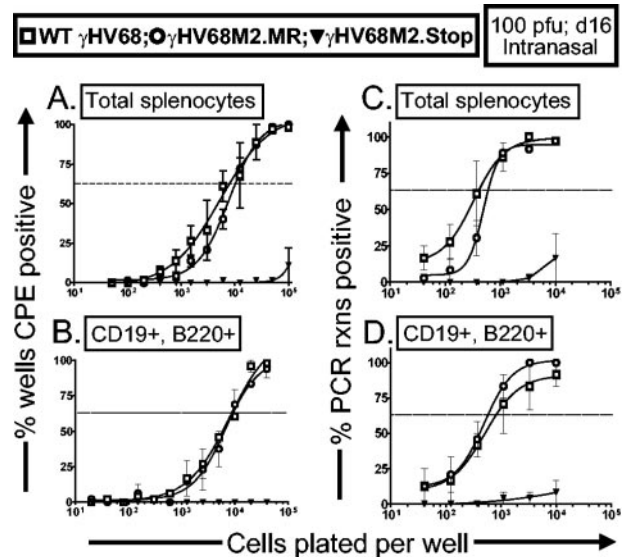


FIG. 3. M2 is required for the establishment of  $\gamma$ HV68 latency in the spleen following intranasal inoculation with 100 PFU. C57BL/6 mice were infected intranasally with 100 PFU of  $\gamma$ HV68M2.Stop,  $\gamma$ HV68M2.MR, or wt  $\gamma$ HV68, and spleens were harvested at 16 dpi (d16). Splenic B cells (CD19<sup>+</sup> B220<sup>+</sup>) were purified by FACS as described in Materials and Methods (Fig. 2). Bulk splenocytes and isolated B cells were analyzed by limiting-dilution ex vivo reactivation assays and limiting-dilution viral genome PCR assays. (A) Frequency of unsorted splenocytes reactivating virus. (B) Frequency of FACS-purified splenic B cells reactivating virus. (C) Frequency of unsorted splenocytes harboring the viral genome. (D) Frequency of FACS-purified splenic B cells harboring the viral genome. For the limiting-dilution ex vivo reactivation assays (A and B), live, intact splenocytes or B cells were serially diluted on MEF indicator monolayers in parallel with mechanically disrupted samples in order to distinguish between virus reactivated from latency and preformed infectious virus. In this report, no preformed infectious virus of any of the strains assayed was detected; hence, for clarity, these data are not shown. For each sample dilution, 24 wells were scored for the presence of CPEs (see Materials and Methods). Limiting-dilution PCR assays were used to determine the frequency of bulk splenocytes or B cells harboring the viral genome (C and D). Samples were serially diluted into a background of  $10^4$  uninfected cells, lysed, and subjected to nested PCR to detect the viral genome (see Materials and Methods). Data are expressed as the mean  $\pm$  standard error of the mean percentage of wells positive for virus (CPE or viral DNA). Curve fit lines for both assays were derived from nonlinear regression analysis. The horizontal line indicates 63.2%, from which the frequency of cells reactivating virus or the frequency of cells harboring the viral genome was determined based on the Poisson distribution. The data shown are from three independent experiments.

cells (1 in 1,480 unsorted splenocytes) from the spleens of mice infected with  $\gamma$ HV68M2.Stop carried the viral genome (Fig. 4C and D and Table 2). These data demonstrate that increasing the dose can facilitate the establishment of latency in splenic B cells by the M2 mutant virus, but at reduced levels. In addition, examination of reactivation from latency revealed a severe defect in the ability of the M2 mutant virus to reactivate from B cells (Fig. 4A and B). The frequency of splenic B-cell reactivation in mice infected with  $\gamma$ HV68M2.Stop was too low to be accurately determined compared to splenic B-cell reactivation in mice infected with wt  $\gamma$ HV68 or  $\gamma$ HV68M2.MR (1 in 9,200 and 1 in 5,975, respectively) (Fig. 4A and B and Table 1).

TABLE 1. Frequencies of ex vivo unsorted splenocytes and splenic B cells showing reactivation from latency at 16 dpi

| Virus                | Route of infection <sup>a</sup> | Dose for infection (PFU) | Cell population  | Frequency of cells showing reactivation (1 in) <sup>b</sup> | Total no. of cells <sup>c</sup> | No. of cells showing reactivation <sup>d</sup> |
|----------------------|---------------------------------|--------------------------|------------------|---|---------------------------------|--|
| wt $\gamma$ HV68     | i.n.                            | 100                      | Unsorted B cells | 8,072   | $9.52 \times 10^7$              | 11,794   |
|                      |                                 |                          |                  | 8,800   | $3.90 \times 10^7$              | 4,432  |
| $\gamma$ HV68M2.MR   | i.n.                            | 100                      | Unsorted B cells | 10,400  | $1.10 \times 10^8$              | 10,577   |
|                      |                                 |                          |                  | 9,200   | $4.62 \times 10^7$              | 5,022  |
| $\gamma$ HV68M2.Stop | i.n.                            | 100                      | Unsorted B cells | ND  | $7.28 \times 10^7$              | NA   |
|                      |                                 |                          |                  | ND  | $3.57 \times 10^7$              | NA   |
| wt $\gamma$ HV68     | i.n.                            | $4 \times 10^5$          | Unsorted B cells | 12,600  | $9.42 \times 10^7$              | 7,476  |
|                      |                                 |                          |                  | 9,200   | $3.86 \times 10^7$              | 4,196  |
| $\gamma$ HV68M2.MR   | i.n.                            | $4 \times 10^5$          | Unsorted B cells | 6,775   | $1.26 \times 10^8$              | 18,598   |
|                      |                                 |                          |                  | 5,975   | $5.29 \times 10^7$              | 8,854  |
| $\gamma$ HV68M2.Stop | i.n.                            | $4 \times 10^5$          | Unsorted B cells | ND  | $8.06 \times 10^7$              | NA   |
|                      |                                 |                          |                  | ND  | $3.95 \times 10^7$              | NA   |
| wt $\gamma$ HV68     | i.p.                            | 100                      | Unsorted B cells | 5,650   | $1.30 \times 10^8$              | 23,009   |
|                      |                                 |                          |                  | 7,900   | $5.3 \times 10^7$               | 6,747  |
| $\gamma$ HV68M2.MR   | i.p.                            | 100                      | Unsorted B cells | 16,900  | $9.30 \times 10^7$              | 5,503  |
|                      |                                 |                          |                  | 13,100  | $3.91 \times 10^7$              | 2,985  |
| $\gamma$ HV68M2.Stop | i.p.                            | 100                      | Unsorted B cells | ND  | $7.84 \times 10^7$              | NA   |
|                      |                                 |                          |                  | ND  | $3.84 \times 10^7$              | NA   |

<sup>a</sup> i.n., intranasal; i.p., intraperitoneal.

<sup>b</sup> Determined from the mean of at least three independent experiments with splenocytes pooled from five mice per experimental group. ND, not determined (values were below the limit of detection of the assay).

<sup>c</sup> B-cell numbers were derived from the total number of unsorted cells per spleen for each virus, dose of infection, route of infection, and percentage of total spleen cells represented by this population, as calculated by FACS gating (see the legend to Fig. 2).

<sup>d</sup> Derived from the experimental frequency data and the approximate total number of cells per population. NA, not applicable, due to the inability to accurately determine the frequency of cells showing reactivation.

### M2 is required for $\gamma$ HV68 reactivation from latency in splenic B cells following low-dose intraperitoneal inoculation.

In contrast to the results obtained after intranasal inoculation, M2 was previously shown to be dispensable for splenic latency and reactivation at early times following intraperitoneal inoculation with  $10^6$  PFU of virus (11). To assess whether the dose of infection contributes to the ability of the M2 mutant virus to establish and reactivate from latency in the spleen, mice were infected intraperitoneally with 100 PFU of wt  $\gamma$ HV68,  $\gamma$ HV68M2.MR, or  $\gamma$ HV68M2.Stop. At 16 dpi, splenic B cells (CD19<sup>+</sup> B220<sup>+</sup>) and unsorted splenocytes were harvested and subjected to a limiting-dilution ex vivo reactivation assay (Fig. 5A and B). In the bulk splenocyte population, significant reactivation was observed for both wt and  $\gamma$ HV68M2.MR viruses (1 in 5,650 and 1 in 16,900, respectively). However, significantly lower reactivation was observed for the M2 mutant virus (<1 in 100,000) (Fig. 5A and B). When reactivation from purified B cells was examined, nearly equivalent frequencies of reactivation were observed for wt and  $\gamma$ HV68M2.MR viruses (1 in 7,900 and 1 in 13,100, respectively), while nearly undetectable levels of reactivation were observed for  $\gamma$ HV68M2.Stop mutant virus (Fig. 5A and B). However, when the frequencies of cells harboring the viral genome were assessed, the presence of M2 mutant virus in infected splenocytes was readily detected (1 in 530 total splenocytes and 1 in 500 purified B cells). These values are slightly lower than those for wt and marker rescue

viruses, which were present at ca. four- or fivefold higher levels (Fig. 5C and D and Table 2).

Importantly, with regard to intraperitoneal infection, it is clear that the modest defect in the establishment of latency in B cells cannot account for the severe defect in reactivation from latency. We hypothesize that non-B cells harboring latent  $\gamma$ HV68M2.Stop contribute to the small amount of reactivation which was observed in bulk splenocytes (Fig. 5A) but which was not apparent in the purified B-cell population. In addition, these studies show that the establishment of latency in splenic B cells is a route of the infection-dependent M2 mutant virus phenotype.

**slgD<sup>+</sup> splenic B cells harbor increased frequencies of M2 mutant virus at late times postinfection following intraperitoneal inoculation.**  $\gamma$ HV68 long-term latency is largely confined to isotype-switched memory B cells (9, 37). With regard to EBV persistence, it has been hypothesized that latently infected memory B cells are capable of leaving the site of acute-phase replication (tonsils) and circulating through the peripheral blood, allowing the virus to spread itself to secondary lymphoid organs, such as the spleen (26). As described above, the M2 mutant virus has a severe defect in the establishment of latency in the spleen following intranasal inoculation. Given the ability of  $\gamma$ HV68M2.Stop to establish latency in splenic B cells following low-dose intraperitoneal inoculation, this route of infection was used to investigate whether the failure of

TABLE 2. Frequencies of unsorted splenocytes and splenic B cells harboring viral genomes at 16 dpi

| Virus                | Route of infection <sup>a</sup> | Dose for infection (PFU) | Cell population | Frequencies of viral genome-positive cells (1 in) <sup>b</sup> | Total no. of cells <sup>c</sup> | Total no. of genome-positive cells <sup>d</sup> |
|----------------------|---------------------------------|--------------------------|-----------------|--|---------------------------------|---|
| wt $\gamma$ HV68     | i.n.                            | 100                      | Unsorted        | 406  | $9.52 \times 10^7$              | 234,483   |
|                      |                                 |                          |                 | 820  | $3.90 \times 10^7$              | 47,561  |
| $\gamma$ HV68M2.MR   | i.n.                            | 100                      | Unsorted        | 600  | $1.10 \times 10^8$              | 183,333   |
|                      |                                 |                          |                 | 580  | $4.62 \times 10^7$              | 79,655  |
| $\gamma$ HV68M2.Stop | i.n.                            | 100                      | Unsorted        | ND   | $7.28 \times 10^7$              | NA  |
|                      |                                 |                          |                 | ND   | $3.57 \times 10^7$              | NA  |
| wt $\gamma$ HV68     | i.n.                            | $4 \times 10^5$          | Unsorted        | 305  | $9.42 \times 10^7$              | 308,852   |
|                      |                                 |                          |                 | 467  | $3.86 \times 10^7$              | 82,655  |
| $\gamma$ HV68M2.MR   | i.n.                            | $4 \times 10^5$          | Unsorted        | 145  | $1.26 \times 10^8$              | 868,965   |
|                      |                                 |                          |                 | 285  | $5.29 \times 10^7$              | 185,614   |
| $\gamma$ HV68M2.Stop | i.n.                            | $4 \times 10^5$          | Unsorted        | 1,480  | $8.06 \times 10^7$              | 54,459  |
|                      |                                 |                          |                 | 2,100  | $3.95 \times 10^7$              | 18,809  |
| wt $\gamma$ HV68     | i.p.                            | 100                      | Unsorted        | 140  | $1.30 \times 10^8$              | 928,571   |
|                      |                                 |                          |                 | 126  | $5.33 \times 10^7$              | 423,016   |
| $\gamma$ HV68M2.MR   | i.p.                            | 100                      | Unsorted        | 190  | $9.30 \times 10^7$              | 489,474   |
|                      |                                 |                          |                 | 183  | $3.91 \times 10^7$              | 213,661   |
| $\gamma$ HV68M2.Stop | i.p.                            | 100                      | Unsorted        | 530  | $7.84 \times 10^7$              | 147,924   |
|                      |                                 |                          |                 | 500  | $3.84 \times 10^7$              | 76,800  |

<sup>a</sup> i.n., intranasal; i.p., intraperitoneal.

<sup>b</sup> Determined from the mean of at least three independent experiments with splenocytes pooled from five mice per experimental group. ND, not determined (values were below the limit of detection of the assay).

<sup>c</sup> B-cell numbers were derived from the total number of unsorted cells per spleen for each virus, dose of infection, route of infection, and percentage of total spleen cells represented by this population, as calculated by FACS gating (see the legend to Fig. 2).

<sup>d</sup> Derived from the experimental frequency data and the approximate total number of cells per population. NA, not applicable, due to the inability to accurately determine the frequency of viral genome-positive cells.

$\gamma$ HV68M2.Stop to establish latency in the spleen at 16 dpi following low-dose intranasal inoculation was due to a defect in the establishment of latency in a specific population of B cells (perhaps responsible for trafficking of the virus from the lungs to the spleen after intranasal infection).

Mice were infected with either  $\gamma$ HV68M2.Stop or  $\gamma$ HV68M2.MR and, at various times postinfection, mature B cells lacking sIgD (sIgD negative [sIgD<sup>-</sup>]) and naive B cells (CD19<sup>+</sup> sIgD positive [sIgD<sup>+</sup>]) were purified by flow cytometry (Fig. 6). At 16 dpi, the frequency of viral genome-positive naive B cells isolated from mice infected with  $\gamma$ HV68M2.MR was 1 in 4,000, whereas the frequency of viral genome-positive sIgD<sup>-</sup> B cells was 1 in 148, as determined by a limiting-dilution PCR assay (Fig. 7 and Table 3). In contrast, the frequency of naive B cells harboring the viral genome from mice infected with  $\gamma$ HV68M2.Stop was lower than that for marker rescue virus at day 16 (ca. 1 in 17,000). However, the frequency of viral genome-positive sIgD<sup>-</sup> B cells was nearly the same as that seen with  $\gamma$ HV68M2.MR infection, at 1 in 164 (Table 3). At 42 dpi, the frequency of viral genome-positive naive B cells purified from  $\gamma$ HV68M2.Stop-infected mice was over 50-fold higher than that seen with  $\gamma$ HV68M2.MR infection (Fig. 7). Again, the frequencies of viral genome-positive sIgD<sup>-</sup> B cells were similar in  $\gamma$ HV68M2.Stop and  $\gamma$ HV68M2.MR infections (Table 3). To complete the time course, the establishment of latency was examined at 6 months postinfection. As at early

time points, the levels of viral genome-positive sIgD<sup>-</sup> B cells in the spleen were similar in  $\gamma$ HV68M2.MR and  $\gamma$ HV68M2.Stop infections. However, a significantly higher level of the viral genome was found in naive splenic B cells at 6 months after infection with  $\gamma$ HV68M2.Stop than after infection with  $\gamma$ HV68M2.MR (Table 3 and Fig. 7).

These analyses suggested that  $\gamma$ HV68M2.Stop has no defect in the establishment of latency in memory B cells, which represent a  $\gamma$ HV68 long-term latency reservoir in the spleen. However, the loss of sIgD from B cells does not conclusively indicate that these cells are bona fide memory B cells, identified by the surface expression of either sIgM or isotype-switched immunoglobulin (IgG, IgA, and IgE). To investigate the possibility that  $\gamma$ HV68M2.Stop persistence was maintained in a subset of immature B cells lacking sIgD expression, the spleens of mice infected with either  $\gamma$ HV68M2.Stop or  $\gamma$ HV68M2.MR were harvested at 42 dpi, and isotype-switched CD19<sup>+</sup> B cells were isolated by FACS with a cocktail of antibodies (IgG1, IgG2a, IgG2b, IgG3, IgA, and IgE). As in sIgD<sup>-</sup> B cells in the spleen,  $\gamma$ HV68M2.Stop was present in isotype-switched B cells at a frequency of approximately 1 in 65 cells, and  $\gamma$ HV68M2.MR was found at a frequency of 1 in 145 cells (Table 3). These results indicate that  $\gamma$ HV68M2.Stop, like wt  $\gamma$ HV68, is capable of establishing latency in isotype-switched memory B cells.

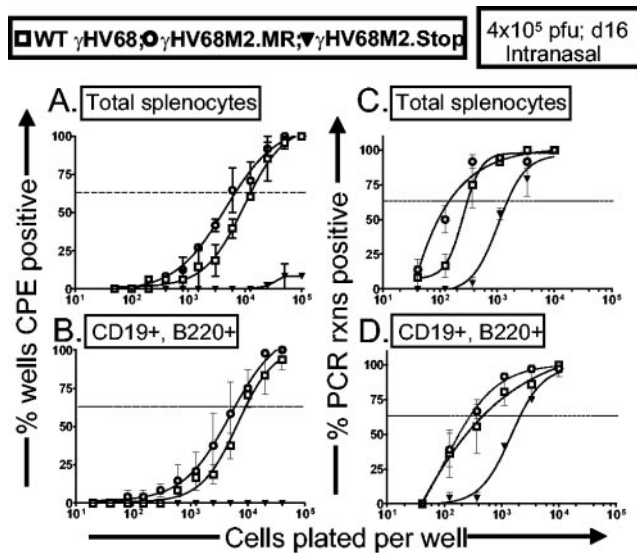


FIG. 4. M2 is required for  $\gamma$ HV68 reactivation from latency in splenic B cells following intranasal inoculation with  $4 \times 10^5$  PFU. C57BL/6 mice were infected intranasally with  $4 \times 10^5$  PFU of  $\gamma$ HV68M2.Stop,  $\gamma$ HV68M2.MR, or wt  $\gamma$ HV68, and spleens were harvested at 16 dpi (d16). Splenic B cells ( $CD19^+ B220^+$ ) were purified by FACS as described in Materials and Methods (Fig. 2). Bulk splenocytes and isolated B cells were analyzed by limiting-dilution ex vivo reactivation assays and limiting-dilution viral genome PCR assays. (A) Frequency of unsorted splenocytes reactivating virus. (B) Frequency of FACS-purified splenic B cells reactivating virus. (C) Frequency of unsorted splenocytes harboring the viral genome. (D) Frequency of FACS-purified splenic B cells harboring the viral genome. The limiting-dilution ex vivo reactivation assays (A and B) and the limiting-dilution PCR assays (C and D) are described in the legend to Fig. 3 and in Materials and Methods. Data are expressed as the mean  $\pm$  standard error of the mean percentage of wells positive for virus (CPE or viral DNA). Curve fit lines for both assays were derived from nonlinear regression analysis. The horizontal line indicates 63.2%, from which the frequency of cells reactivating virus or the frequency of cells harboring the viral genome was determined based on the Poisson distribution. The data shown are from three independent experiments.

**At late times following low-dose intranasal inoculation, M2 mutant virus is present in splenic B cells.** As described above, the M2 mutant virus was incapable of establishing latency at a detectable level in the spleen at 16 dpi following low-dose intranasal inoculation. To investigate whether this absence of latency in the spleen extended to later times postinfection, mice were infected intranasally with 100 PFU of either  $\gamma$ HV68M2.Stop or  $\gamma$ HV68M2.MR, and splenocytes were harvested at 42 dpi and 3 months postinfection. At 42 dpi, splenic B cells ( $CD19^+ B220^+$ ) isolated from mice infected with  $\gamma$ HV68M2.MR harbored the viral genome at a frequency of 1 in 542 cells (Fig. 8 and Table 3). In addition, a low level of M2 mutant virus was apparent in purified splenic B cells ( $<1$  in 10,000) (Fig. 8).

To determine whether wild-type levels of latency were achieved by the M2 mutant virus at later times postinfection, we assessed the presence of the viral genome in the spleens of infected mice at 3 months postinfection. Surprisingly, the frequency of cells harboring the M2 mutant virus (both in unfractionated splenocytes and in purified  $IgD^-$  B cells) was nearly identical to that seen with the M2 marker rescue virus (Fig. 8

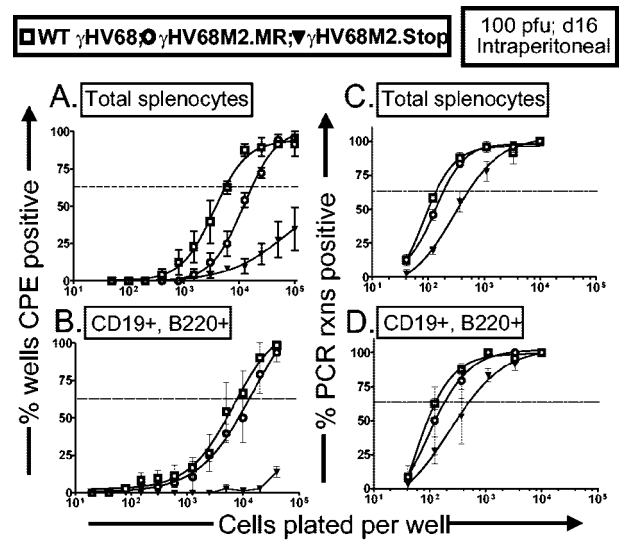


FIG. 5. M2 is required for  $\gamma$ HV68 reactivation from latency in splenic B cells following intraperitoneal inoculation with 100 PFU. C57BL/6 mice were infected intraperitoneally with 100 PFU of  $\gamma$ HV68M2.Stop,  $\gamma$ HV68M2.MR, or wt  $\gamma$ HV68, and spleens were harvested at 16 dpi (d16). Splenic B cells ( $CD19^+ B220^+$ ) were purified by FACS as described in Materials and Methods (Fig. 2). Bulk splenocytes and isolated B cells were analyzed by limiting-dilution ex vivo reactivation assays and limiting-dilution viral genome PCR assays. (A) Frequency of unsorted splenocytes reactivating virus. (B) Frequency of FACS-purified splenic B cells reactivating virus. (C) Frequency of unsorted splenocytes harboring the viral genome. (D) Frequency of FACS-purified splenic B cells harboring the viral genome. The limiting-dilution ex vivo reactivation assays (A and B) and the limiting-dilution PCR assays (C and D) are described in the legend to Fig. 3 and in Materials and Methods. Data are expressed as the mean  $\pm$  standard error of the mean percentage of wells positive for virus (CPE or viral DNA). Curve fit lines for both assays were derived from nonlinear regression analysis. The horizontal line indicates 63.2%, from which the frequency of cells reactivating virus or the frequency of cells harboring the viral genome was determined based on the Poisson distribution. The data shown are from three independent experiments.

and Table 3). Notably, in contrast to the results obtained after intraperitoneal inoculation, no M2 mutant or M2 marker rescue virus was detected in  $IgD^+$  naive B cells at 3 months postinfection. However, the lack of  $\gamma$ HV68 in naive B cells ( $CD19^+ IgD^+$ ) at later times after intranasal infection with wt virus was previously described by Willer and Speck (37) and was observed here following intranasal and intraperitoneal inoculations with  $\gamma$ HV68M2.MR. Why  $\gamma$ HV68M2.Stop persists for a long time in naive B cells after intraperitoneal inoculation but not after intranasal inoculation is unclear but is of significant interest (Fig. 7 and 8).

To assess the possibility that the viral latency observed at late times after low-dose intranasal inoculation with the M2 mutant virus arose from either in vivo selection for a revertant virus or low-level contamination of the M2 mutant virus stock with wild-type  $\gamma$ HV68, splenocytes from mice infected intranasally with 100 PFU of either  $\gamma$ HV68M2.Stop or  $\gamma$ HV68M2.MR were harvested at 91 dpi. Virus reactivation was stimulated by cross-linking of surface immunoglobulin and CD40 (see Materials and Methods) (13a). The titers of viruses obtained from these cultures were determined, and mice were infected with 100 PFU via intranasal inoculation. At 16 dpi,  $\gamma$ HV68M2.Stop



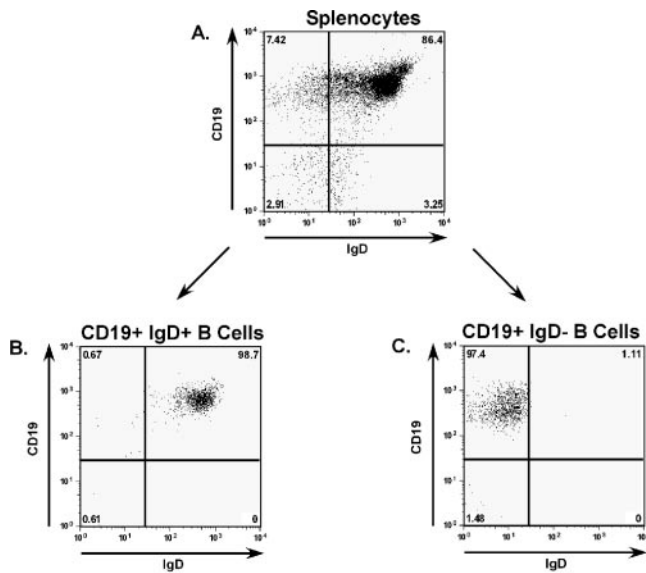


FIG. 6. FACS analysis of surface immunoglobulin staining of sIgD<sup>+</sup> and sIgD<sup>-</sup> splenic B-cell populations. Bulk splenocytes were harvested at 16, 42, 91, or 182 dpi and stained with antibodies directed to CD19 and sIgD. Following staining, samples were subjected to magnetic cell separation as described in Materials and Methods. Flow cytometric dot plots from one representative experiment are shown. (A) Presort analysis of splenocytes. Following magnetic cell separation, the CD19<sup>+</sup> population represented ca. 93.64% ± 1.60% of the total splenocyte population after  $\gamma$ HV68M2.Stop infection and 91.66% ± 4.54% following  $\gamma$ HV68M2.MR infection, regardless of route of infection or dpi. In addition, after  $\gamma$ HV68M2.Stop infection, the CD19<sup>+</sup> sIgD<sup>+</sup> and CD19<sup>+</sup> sIgD<sup>-</sup> subsets represented ca. 84.69% ± 4.21% and 8.95% ± 3.40%, respectively, of the total splenocyte population following magnetic cell separation, regardless of route of infection or dpi. After  $\gamma$ HV68M2.MR infection, the CD19<sup>+</sup> sIgD<sup>+</sup> and CD19<sup>+</sup> sIgD<sup>-</sup> subsets represented ca. 84.64% ± 5.76% and 7.03% ± 1.58%, respectively, of the total splenocyte population following magnetic cell separation, regardless of route of infection or dpi. (B and C) Postsort analyses indicating the purity of fractionated splenic B-cell subsets. The mean purities over 10 experiments were as follows: for  $\gamma$ HV68M2.Stop infection, 98.05% ± 0.56% for CD19<sup>+</sup> sIgD<sup>+</sup> and 94.55% ± 2.33% for CD19<sup>+</sup> sIgD<sup>-</sup> (3.09% ± 2.02% contamination from the CD19<sup>+</sup> sIgD<sup>+</sup> population); and for  $\gamma$ HV68M2.MR infection, 98.38% ± 0.53% for CD19<sup>+</sup> sIgD<sup>+</sup> and 94.49% ± 3.41% for CD19<sup>+</sup> sIgD<sup>-</sup> (2.66% ± 1.85% contamination from the CD19<sup>+</sup> sIgD<sup>+</sup> population).

and  $\gamma$ HV68M2.MR displayed the same splenic latency phenotypes as those observed in previous analyses reported here (data not shown). Thus, we conclude that the latency observed at late times in the spleens of mice reflects the behavior of the M2 mutant virus and not a revertant virus or contaminating wt virus.

## DISCUSSION

Analogous to EBV at early times postinfection,  $\gamma$ HV68 resides within various B-cell subsets while long-term latency is maintained exclusively in memory B cells. The memory compartment represents a long-lived, immunologically privileged reservoir in which  $\gamma$ HV68 and EBV may remain virtually undetected by immune surveillance. In addition, there is a growing body of evidence to support the notion that EBV utilizes memory B cells to traffic from the region of acute-phase rep-

lication to alternate sites of infection within the host (26). It is hypothesized that through the expression of a subset of viral genes, including those for LMP1 and LMP2A, EBV is capable of gaining access to the memory compartment by infecting naive B cells and driving their differentiation into memory B cells (26). By analyzing the impact of  $\gamma$ HV68 latency genes on the establishment of long-term latency in memory B cells, specific  $\gamma$ HV68 genes that could be involved in manipulating B-cell differentiation may be identified. In this report, the contribution of the latency-associated M2 gene to  $\gamma$ HV68 splenic B-cell latency in vivo was evaluated by using a viral recombinant containing a translational stop codon within the M2 ORF.

**Role of M2 in establishing  $\gamma$ HV68 latency in splenic B cells.** Previously, Jacoby et al. (11) have shown that  $\gamma$ HV68 splenic latency was approximately 10-fold lower in mice infected intranasally with  $4 \times 10^5$  PFU of  $\gamma$ HV68M2.Stop than wt  $\gamma$ HV68. However following intraperitoneal inoculation,  $\gamma$ HV68M2.Stop established latency in bulk splenocytes at a comparable level to wt virus. We show here that reducing the inoculating dose of virus administered intranasally revealed a severe defect in the initial establishment of B-cell latency in the spleens of mice in the absence of a functional M2 gene. However, only a modest defect in the early establishment of B-cell latency was detected upon low-dose intraperitoneal inoculation, suggesting route-specific differences in trafficking virus to the spleen. Interestingly, a similar phenotype is observed upon  $\gamma$ HV68 infection of B-cell-deficient mice, where splenic latency is readily established following intraperitoneal inoculation but not following intranasal inoculation (30, 35). Notably, adoptive transfer of uninfected, T cell-depleted splenocytes, facilitates establishment of  $\gamma$ HV68 splenic latency after intranasal inoculation (23). The latter suggests the possibility that trafficking of  $\gamma$ HV68 from the lungs to the spleen requires B cells—perhaps latently infected B cells that reactivate in the spleen, seeding virus replication in the spleen and subsequent establishment of splenic B-cell latency. As such, the severe reactivation defect in latently infected B cells caused by the loss of M2 might result in a failure to seed virus replication and latency in the spleen (Fig. 9). Notably, after intraperitoneal inoculation of the M2 mutant, virus reactivation from latency was observed in explanted bulk splenocytes (Fig. 5A), presumably from non-B cells harboring latent  $\gamma$ HV68M2.Stop. However, following high-dose intranasal inoculation with  $\gamma$ HV68M2.Stop, we did not observe significant virus reactivation from latency in bulk splenocytes (Fig. 4A). A possible explanation of this discrepancy is that following intranasal inoculation there is a requirement for trafficking of latently infected B cells to the spleen and subsequent virus reactivation to seed non-B-cell latency reservoirs in the spleen. Ultimately, however, there are either alternative mechanisms for seeding B-cell latency in the spleen, or the M2 mutant virus reactivation defect is not absolute in vivo, since latency in the spleen is established to nearly wt levels by 3 months after low-dose intranasal infection.

Consistent with the mechanism proposed above, acute virus replication in the spleen lags significantly behind the kinetics of acute virus replication in the lungs (28). Furthermore, acute replication virus in the spleen following intranasal inoculation also appears at significant later times than following virus in-



TABLE 3. Frequencies of unsorted splenocytes and splenic B-cell subsets harboring viral genomes

| Virus                              | Route of infection <sup>a</sup>     | dpi                                 | Cell population                    | Frequencies of viral genome-positive cells (1 in) <sup>b</sup> | Total no. of cells <sup>c</sup> | Total no. of genome-positive cells <sup>d</sup> |
|------------------------------------|-------------------------------------|-------------------------------------|------------------------------------|--|---------------------------------|---|
| $\gamma$ HV68M2.MR                 | i.p.                                | 16                                  | Unsorted                           | 190  | $9.30 \times 10^7$              | 489,474   |
|                                    |                                     |                                     | CD19 <sup>+</sup> IgD <sup>+</sup> | 4,000  | $3.04 \times 10^7$              | 7,600   |
|                                    |                                     |                                     | CD19 <sup>+</sup> IgD <sup>-</sup> | 148  | $2.53 \times 10^6$              | 17,095  |
|                                    |                                     | 42                                  | Unsorted                           | 1,800  | $7.02 \times 10^7$              | 39,000  |
|                                    |                                     |                                     | CD19 <sup>+</sup> IgD <sup>+</sup> | 14,135   | $2.30 \times 10^7$              | 1,627   |
|                                    |                                     |                                     | CD19 <sup>+</sup> IgD <sup>-</sup> | 150  | $1.91 \times 10^6$              | 12,733  |
|                                    | CD19 <sup>+</sup> IgG <sup>+e</sup> |                                     | 145                                | $1.00 \times 10^6$   | 6,922                           |   |
|                                    | CD19 <sup>+</sup> IgG <sup>-e</sup> |                                     | 3,510                              | $2.39 \times 10^7$   | 6,808                           |   |
|                                    | 182                                 | Unsorted                            | 5,300                              | $4.81 \times 10^7$   | 9,075                           |   |
|                                    |                                     | CD19 <sup>+</sup> IgD <sup>+</sup>  | ND                                 | $1.57 \times 10^7$   | NA                              |   |
|                                    |                                     | CD19 <sup>+</sup> IgD <sup>-</sup>  | 355                                | $1.31 \times 10^6$   | 3,690                           |   |
|                                    | $\gamma$ HV68M2.Stop                | i.p.                                | 16                                 | Unsorted   | 530                             | $7.84 \times 10^7$                              |
| CD19 <sup>+</sup> IgD <sup>+</sup> |                                     |                                     |                                    | 17,201   | $3.06 \times 10^7$              | 1,779   |
| CD19 <sup>+</sup> IgD <sup>-</sup> |                                     |                                     |                                    | 164  | $3.23 \times 10^6$              | 19,695  |
| 42                                 |                                     |                                     | Unsorted                           | 330  | $6.03 \times 10^7$              | 182,727   |
|                                    |                                     |                                     | CD19 <sup>+</sup> IgD <sup>+</sup> | 1,390  | $2.35 \times 10^7$              | 16,906  |
|                                    |                                     |                                     | CD19 <sup>+</sup> IgD <sup>-</sup> | 67   | $2.49 \times 10^6$              | 37,164  |
|                                    |                                     | CD19 <sup>+</sup> IgG <sup>+e</sup> | 65                                 | $6.58 \times 10^5$   | 10,127                          |   |
|                                    |                                     | CD19 <sup>+</sup> IgG <sup>-e</sup> | 1,620                              | $2.49 \times 10^7$   | 15,379                          |   |
| 182                                |                                     | Unsorted                            | 3,900                              | $4.19 \times 10^7$   | 10,744                          |   |
|                                    |                                     | CD19 <sup>+</sup> IgD <sup>+</sup>  | 23,536                             | $1.63 \times 10^7$   | 693                             |   |
|                                    |                                     | CD19 <sup>+</sup> IgD <sup>-</sup>  | 255                                | $1.73 \times 10^6$   | 6,784                           |   |
| $\gamma$ HV68M2.MR                 |                                     | i.n.                                | 42                                 | Unsorted   | 653                             | $4.62 \times 10^7$                              |
|                                    | B cells                             |                                     |                                    | 542  | $1.94 \times 10^7$              | 35,793  |
|                                    | 91                                  |                                     | Unsorted                           | 9,400  | $5.11 \times 10^7$              | 5,436   |
|                                    |                                     |                                     | CD19 <sup>+</sup> IgD <sup>+</sup> | ND   | $1.51 \times 10^7$              | NA  |
|                                    |                                     | CD19 <sup>+</sup> IgD <sup>-</sup>  | 890                                | $1.26 \times 10^6$   | 1,416                           |   |
| $\gamma$ HV68M2.Stop               | i.n.                                | 42                                  | Unsorted                           | 26,867   | $4.78 \times 10^7$              | 1,779   |
|                                    |                                     |                                     | B cells                            | 24,061   | $2.34 \times 10^7$              | 972   |
|                                    |                                     | 91                                  | Unsorted                           | 16,906   | $5.88 \times 10^7$              | 3,478   |
|                                    |                                     |                                     | CD19 <sup>+</sup> IgD <sup>+</sup> | ND   | $2.29 \times 10^7$              | NA  |
|                                    |                                     | CD19 <sup>+</sup> IgD <sup>-</sup>  | 580                                | $2.42 \times 10^6$   | 4,172                           |   |

<sup>a</sup> i.p., intraperitoneal; i.n., intranasal.

<sup>b</sup> Determined from the mean of two or three independent experiments with splenocytes pooled from 10 to 15 mice per experimental group. ND, not determined (values were below the limit of detection of the assay).

<sup>c</sup> Cell numbers were derived from the total number of unsorted cells per spleen for each virus, dose of infection, route of infection, and percentage of total spleen cells represented by each subset, as calculated by FACS gating (see the legends to Fig. 2 and 6).

<sup>d</sup> Derived from the experimental frequency data and the approximate total number of cells per population. NA, not applicable, due to the inability to accurately determine the frequency of viral genome-positive cells.

<sup>e</sup> Isotype-switched B cells were stained and purified with a cocktail of antibodies directed against IgG1, IgG2a, IgG2b, IgG3, IgA, and IgE.

fection via intraperitoneal inoculation regardless of dose (28). Thus, the mechanisms involved in seeding virus latency to the spleen following intraperitoneal inoculation may be quite distinct from the mechanisms involved in virus trafficking after intranasal inoculation.

**Role of M2 in the reactivation of virus from latently infected B cells.** The analyses presented here, while demonstrating a route-dependent or dose-dependent delay in the establishment of splenic B-cell latency in the absence of M2, clearly show that M2 is ultimately not required for the establishment of latency in B cells. Furthermore, the M2 mutant virus ultimately ap-

pears to gain access to the memory B-cell reservoir which serves as the major reservoir for maintaining chronic  $\gamma$ HV68 infection. Thus, the major phenotype revealed by these analyses is a severe defect in the ability of B cells latently infected with M2 mutant virus to reactivate from latency. Unfortunately, the mechanisms controlling establishment of  $\gamma$ HV68 latency, and subsequent reactivation from latency, are very poorly understood. Our previous analyses using an ex vivo reactivation assay demonstrated that only a small fraction of viral genome-positive B cells harvested at 16 dpi reactivate, and by 42 dpi very little virus reactivation is observed. Thus, we

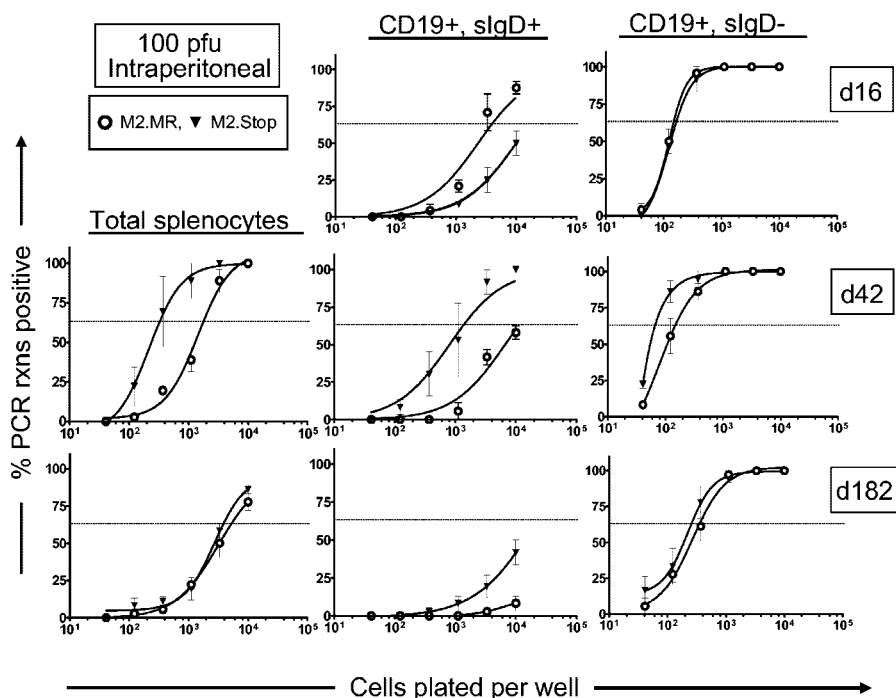


FIG. 7. sIgD<sup>+</sup> splenic B cells harbor an increased frequency of M2 mutant virus at late times postinfection. C57BL/6 mice were infected intraperitoneally with 100 PFU of either  $\gamma$ HV68M2.Stop or  $\gamma$ HV68M2.MR, and spleens were harvested at 16, 42, or 182 dpi (d16, d42, or d182, respectively). Unsorted splenocytes and FACS-purified CD19<sup>+</sup> sIgD<sup>+</sup> and CD19<sup>+</sup> sIgD<sup>-</sup> splenic B cells (Fig. 6 and Materials and Methods) were analyzed by limiting-dilution viral genome PCR assays as described in the legend to Fig. 3 and in Materials and Methods. (Top row) Frequencies of CD19<sup>+</sup> sIgD<sup>+</sup> and CD19<sup>+</sup> sIgD<sup>-</sup> splenic B cells harboring the viral genome at 16 dpi. (Middle row) Frequencies of unsorted splenocytes and CD19<sup>+</sup> sIgD<sup>+</sup> and CD19<sup>+</sup> sIgD<sup>-</sup> splenic B cells harboring the viral genome at 42 dpi. (Bottom row) Frequencies of unsorted splenocytes and CD19<sup>+</sup> sIgD<sup>+</sup> and CD19<sup>+</sup> sIgD<sup>-</sup> splenic B cells harboring the viral genome at 182 dpi. Data are expressed as the mean  $\pm$  standard error of the mean percentage of wells positive for viral DNA. Curve fit lines were derived from nonlinear regression analysis. The horizontal line indicates 63.2%, from which the frequency of cells harboring the viral genome was determined based on the Poisson distribution. The data shown are from two or three independent experiments. rxns, reactions.

have hypothesized that there are substantive changes in virus latency that occur during the first few weeks *in vivo* leading to a form of latency in B cells which does not readily reactivate. We have recently shown that virus reactivation from splenocytes at late times postinfection can be induced by stimulating B cells by cross-linking surface immunoglobulin and CD40 (13a), although only a small percentage of the viral genome-positive B cells can be stimulated to produce virus. Whether all viral genome-positive splenic B cells can reactivate virus remains an open question. It is formally possible that only a subset of the cells harboring viral genomes is actually competent for virus reactivation. If true, this would raise the question of whether the other viral genome-positive cells actually contribute to the maintenance of chronic infection, or represent “dead-end” forms of infection and/or remnants of virus infection.

Why does virus reactivation diminish with time postinfection? One possibility is that the viral genome is targeted for methylation by the host cell-directed *de novo* methylation machinery, resulting in the suppression of key reactivation genes. Viral genome methylation is thought to play a major role in modulating expression of EBV latency-associated genes in latently infected memory B cells in normal seropositive individuals (16, 17). Alternatively, reactivation may be confined to a specific subpopulation of latently infected B cells which are

only transiently present during the establishment of latency *in vivo*. An extension of the latter possibility is that specific  $\gamma$ HV68 latency-associated gene products may play a role in dictating the efficiency of virus reactivation in the *ex vivo* assay, and changes in their expression patterns lead to changes in virus reactivation. Ultimately, any of these changes may lead to a state of the viral genome which requires specific signals to trigger virus reactivation; signals which are not present in the *ex vivo* reactivation assay (e.g., antigen stimulation). The failure to observe significant reactivation from B cells latently infected with M2 mutant virus could reflect (i) the absence of M2 mutant virus in a specific subpopulation of B cells that gives rise to the virus reactivation observed in the *ex vivo* reactivation assay or (ii) that M2 plays a direct role in virus reactivation.

**Role of M2 in the establishment of  $\gamma$ HV68 latency in specific B-cell subsets in the spleen at late times postinfection.** Both EBV and  $\gamma$ HV68 reside within various B-cell populations at early times postinfection, while long-term latency is maintained in memory B cells. For EBV it appears that it has evolved mechanisms to manipulate B-cell differentiation, thereby gaining access to the memory B-cell reservoir. Once the virus has gained access to memory B cells, the virus utilizes these cells to spread throughout the host, invading secondary lymphoid organs including the spleen (26). Given the similar-

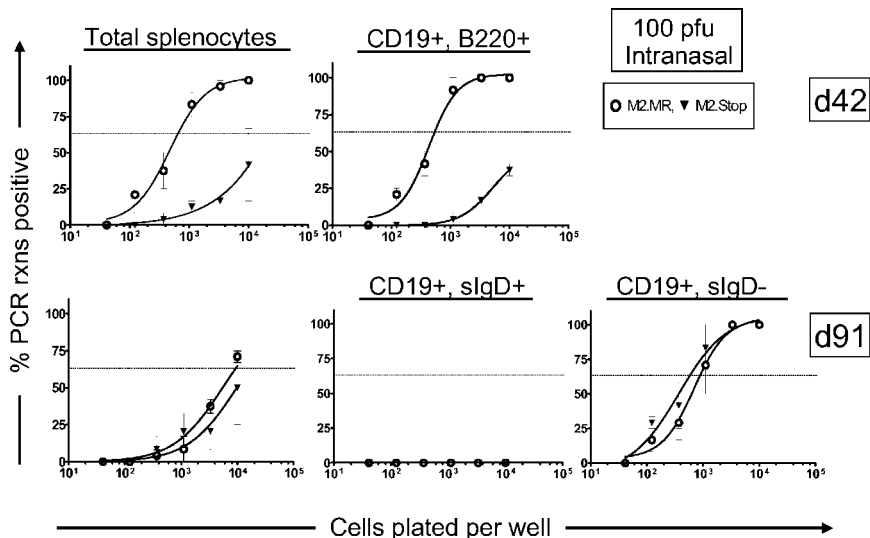


FIG. 8. M2 mutant virus is present in splenic B cells at late times postinfection following low-dose intranasal inoculation. C57BL/6 mice were infected intranasally with 100 PFU of either  $\gamma$ HV68M2.Stop or  $\gamma$ HV68M2.MR, and spleens were harvested at 42 or 91 dpi (d42 or d91, respectively). Splenic B cells (CD19<sup>+</sup> B220<sup>+</sup>) were purified by FACS as described in Materials and Methods at 42 dpi (Fig. 2), and CD19<sup>+</sup> sIgD<sup>+</sup> and CD19<sup>+</sup> sIgD<sup>-</sup> splenic B cells were purified at 3 months postinfection (Fig. 6). Bulk splenocytes and isolated B cells were analyzed by limiting-dilution viral genome PCR assays as described in the legend to Fig. 3 and in Materials and Methods. (Top row) Frequencies of unsorted splenocytes and FACS-purified splenic B cells harboring the viral genome at 42 dpi. (Bottom row) Frequencies of unsorted splenocytes and CD19<sup>+</sup> sIgD<sup>+</sup> and CD19<sup>+</sup> sIgD<sup>-</sup> splenic B cells harboring the viral genome at 3 months postinfection. Data are expressed as the mean  $\pm$  standard error of the mean percentage of wells positive for viral DNA. Curve fit lines were derived from nonlinear regression analysis. The horizontal line indicates 63.2%, from which the frequency of cells harboring the viral genome was determined based on the Poisson distribution. The data shown are from two or three independent experiments. rxns, reactions.

ities between  $\gamma$ HV68 and EBV, it is attractive to speculate that a similar strategy is employed by  $\gamma$ HV68 (Fig. 9). Based on the ability of  $\gamma$ HV68M2.Stop to establish latency in B cells following intraperitoneal inoculation with 100 PFU (Fig. 5), this route of infection was used to investigate the hypothesis that M2 is required for the establishment of latency in a specific subset of B cells that are necessary for trafficking the virus from the lungs to the spleen following intranasal inoculation.

Naive B cells (CD19<sup>+</sup> sIgD<sup>+</sup>) and sIgD<sup>-</sup> B cells were isolated from the spleens of mice infected with either  $\gamma$ HV68M2.Stop or  $\gamma$ HV68M2.MR and examined for the presence of viral genomes. Strikingly, at 42 dpi the frequency of naive B cells harboring the viral genome purified from mice infected with  $\gamma$ HV68M2.Stop was >10-fold higher than that of naive B cells isolated from  $\gamma$ HV68M2.MR-infected animals (Fig. 7 and Table 3). Recently, we showed that the majority  $\gamma$ HV68 latency in the spleen at 16 dpi and at 42 dpi is found in proliferating B cells (Moser et al., unpublished). Thus, the increase in latent virus infection of naive B cells from 16 dpi to 42 dpi in  $\gamma$ HV68M2.Stop-infected mice may reflect proliferation of this latently infected population of B cells, perhaps driven by  $\gamma$ HV68 infection. The failure to observe this expansion in wt  $\gamma$ HV68-infected mice may reflect an M2-dependent differentiation of latently infected naive B cells, and as such, in the absence of M2 expression, there is an accumulation of latently infected naive B cells. Alternatively, this slow decay of latent virus infection of naive B cells upon infection with  $\gamma$ HV68M2.Stop may represent (i) a steady influx of latently infected naive B cells to the spleen from an alternate site of  $\gamma$ HV68 latency; (ii) virus reactivation from B-cell and/or non-B-cell latency reservoirs in the spleen, undetectable by the

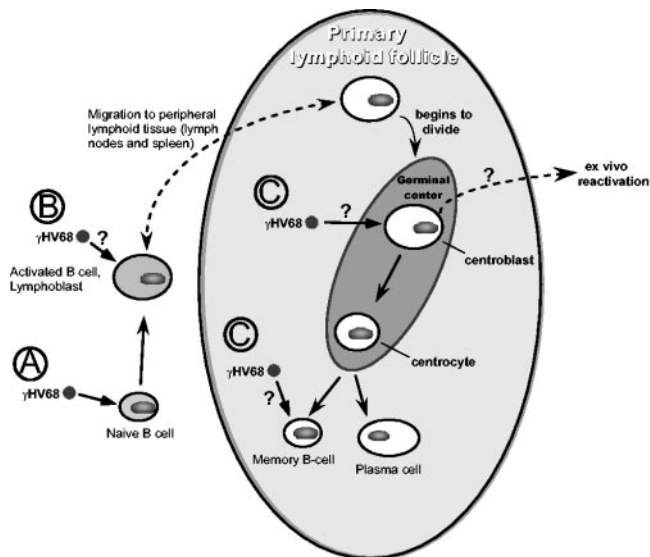


FIG. 9. Mechanisms through which  $\gamma$ HV68 may access memory B cells. As has been proposed for EBV,  $\gamma$ HV68 infection of naive B cells (CD19<sup>+</sup> sIgD<sup>+</sup>) may lead to virus-driven B-cell differentiation, resulting in the establishment of long-term latency in memory B cells (A). Alternatively, under certain experimental conditions (e.g., high-dose infection and/or systemic infection via intraperitoneal inoculation), passive access to the memory B-cell reservoir may occur through  $\gamma$ HV68 infection of antigen-activated naive B cells (B) and/or direct infection of either germinal-center or memory B cells (C). Actively dividing CD19<sup>+</sup> sIgD<sup>-</sup> germinal-center B cells account for a significant proportion of the  $\gamma$ HV68 reactivation observed in the ex vivo reactivation assay (37; Moser and Speck, unpublished). In vivo, virus reactivation from GC B cells may be required for reseeding of latency reservoirs.



limiting-dilution ex vivo reactivation assay; and/or (iii) an inability of the immune system to clear these cells. Regarding the latter, M2 contains a classic *H-2K<sup>d</sup>* epitope which has been shown to be recognized by CD8<sup>+</sup> T cells from  $\gamma$ HV68-infected BALB/c mice (10). However, CD8<sup>+</sup>-T-cell recognition of M2 has not been confirmed in C57BL/6J mice.

By 42 dpi the majority of  $\gamma$ HV68M2.MR, as previously shown for wt  $\gamma$ HV68 (9, 37), was found in sIgD<sup>-</sup> B cells (germinal center and memory B cells), and only about 10% of the virus was present in naive B cells (ca. 1 in 10,000 naive B cells). In contrast, the frequency of naive B cells latently infected with M2 mutant virus increased from <1 in 10,000 to ca. 1 in 1,000 by 42 dpi. Even by 6 months postinfection,  $\gamma$ HV68-infected naive B cells were still detectable. It is unclear whether the altered kinetics of decay of  $\gamma$ HV68 infected naive B cells reflects an inability of M2 mutant virus to drive the differentiation of these cells and/or reseeding infection of naive B cells due to increased virus reactivation in the lungs and/or non-B-cell latency reservoirs. Notably, the frequency of CD19<sup>+</sup> sIgD<sup>-</sup> B cells was nearly identical in M2 mutant and marker rescue virus infected mice at all time assessed following interperitoneal inoculation. However, although the frequency of viral genome-positive sIgD<sup>-</sup> B cells are approximately equivalent for  $\gamma$ HV68M2.MR and  $\gamma$ HV68M2.Stop, we do not know the relative contribution to this reservoir from (i) virus-driven B-cell differentiation; (ii) passive access through infection of antigen-activated naive B cells; and/or (iii) direct infection of existing GC or memory B cells (Fig. 9). Indeed, this represents one of the central unresolved issues in  $\gamma$ HV68 pathogenesis.

**Conclusion.** We have shown here that the loss of M2 leads to route- and dose-specific defects in the early establishment of  $\gamma$ HV68 latency in splenic B cells. In addition, experimental conditions that lead to the early establishment of splenic latency with M2 mutant virus also demonstrate a critical role of M2 in virus reactivation. Ultimately, however, the M2 mutant virus is able to gain access to the IgD<sup>-</sup>B-cell reservoir following either intraperitoneal or intranasal infection. It seems reasonable to speculate that in the context of natural infection, the M2 gene product plays a critical role in establishing chronic infection. Further understanding of the role of M2 in chronic infection will require insights into the function of this viral antigen. M2 lacks any discernible homology to any known cellular or pathogen proteins but does contain several PxxP motifs that can interact with some SH3 domain-containing proteins (M. Jacoby and S. H. Speck, unpublished data). We are presently determining the importance of these interactions to M2 function during the course of virus infection.

#### ACKNOWLEDGMENTS

This research was supported by NIH grants R01 CA43143, R01 CA95318, and R01 AI58057 to S.H.S.

We thank Robert E. Karaffa II for cell sorting and analysis and members of the Speck Laboratory for helpful comments and discussions.

#### REFERENCES

- Blaskovic, D., M. Stancekova, J. Svobodova, and J. Mistrikova. 1980. Isolation of five strains of herpesviruses from two species of free living small rodents. *Acta Virol.* **24**:468.
- Clambey, E. T., H. W. T. Virgin, and S. H. Speck. 2002. Characterization of a spontaneous 9.5-kilobase-deletion mutant of murine gammaherpesvirus 68 reveals tissue-specific genetic requirements for latency. *J. Virol.* **76**:6532–6544.
- Doherty, P. C., J. P. Christensen, G. T. Belz, P. G. Stevenson, and M. Y. Sangster. 2001. Dissecting the host response to a gamma-herpesvirus. *Philos. Trans. R. Soc. Lond. B* **356**:581–593.
- Doherty, P. C., R. A. Tripp, A. M. Hamilton-Easton, R. D. Cardin, D. L. Woodland, and M. A. Blackman. 1997. Tuning into immunological dissonance: an experimental model for infectious mononucleosis. *Curr. Opin. Immunol.* **9**:477–483.
- Efstathiou, S., Y. M. Ho, S. Hall, C. J. Styles, S. D. Scott, and U. A. Gompels. 1990. Murine herpesvirus 68 is genetically related to the gammaherpesviruses Epstein-Barr virus and herpesvirus saimiri. *J. Gen. Virol.* **71**:1365–1372.
- Efstathiou, S., Y. M. Ho, and A. C. Minson. 1990. Cloning and molecular characterization of the murine herpesvirus 68 genome. *J. Gen. Virol.* **71**:1355–1364.
- Ehtisham, S., N. P. Sunil-Chandra, and A. A. Nash. 1993. Pathogenesis of murine gammaherpesvirus infection in mice deficient in CD4 and CD8 T cells. *J. Virol.* **67**:5247–5252.
- Flano, E., S. M. Husain, J. T. Sample, D. L. Woodland, and M. A. Blackman. 2000. Latent murine gamma-herpesvirus infection is established in activated B cells, dendritic cells, and macrophages. *J. Immunol.* **165**:1074–1081.
- Flano, E., I. J. Kim, D. L. Woodland, and M. A. Blackman. 2002. Gamma-herpesvirus latency is preferentially maintained in splenic germinal center and memory B cells. *J. Exp. Med.* **196**:1363–1372.
- Husain, S. M., E. J. Usherwood, H. Dyson, C. Coleclough, M. A. Coppola, D. L. Woodland, M. A. Blackman, J. P. Stewart, and J. T. Sample. 1999. Murine gammaherpesvirus M2 gene is latency-associated and its protein a target for CD8(+) T lymphocytes. *Proc. Natl. Acad. Sci. USA* **96**:7508–7513.
- Jacoby, M. A., H. W. T. Virgin, and S. H. Speck. 2002. Disruption of the M2 gene of murine gammaherpesvirus 68 alters splenic latency following intranasal, but not intraperitoneal, inoculation. *J. Virol.* **76**:1790–1801.
- Macrae, A. I., E. J. Usherwood, S. M. Husain, E. Flano, I. J. Kim, D. L. Woodland, A. A. Nash, M. A. Blackman, J. T. Sample, and J. P. Stewart. 2003. Murid herpesvirus 4 strain 68 M2 protein is a B-cell-associated antigen important for latency but not lymphocytosis. *J. Virol.* **77**:9700–9709.
- Mistrikova, J., and D. Blaskovic. 1985. Ecology of the murine alphaherpesvirus and its isolation from lungs of rodents in cell culture. *Acta Virol.* **29**:312–317.
- Moser, J. M., J. W. Upton, K. S. Gray, and S. H. Speck. Ex vivo stimulation of gammaherpesvirus 68 latently infected B cells triggers reactivation from latency. *J. Virol.*, in press.
- Nash, A. A., B. M. Dutia, J. P. Stewart, and A. J. Davison. 2001. Natural history of murine gamma-herpesvirus infection. *Philos. Trans. R. Soc. Lond. B* **356**:569–579.
- Nash, A. A., and N. P. Sunil-Chandra. 1994. Interactions of the murine gammaherpesvirus with the immune system. *Curr. Opin. Immunol.* **6**:560–563.
- Paulson, E. J., J. D. Fingerth, J. L. Yates, and S. H. Speck. 2002. Methylation of the EBV genome and establishment of restricted latency in low-passage EBV-infected 293 epithelial cells. *Virology* **299**:109–121.
- Paulson, E. J., and S. H. Speck. 1999. Differential methylation of Epstein-Barr virus latency promoters facilitates viral persistence in healthy seropositive individuals. *J. Virol.* **73**:9959–9968.
- Pollock, J. L., and H. W. T. Virgin. 1995. Latency, without persistence, of murine cytomegalovirus in the spleen and kidney. *J. Virol.* **69**:1762–1768.
- Rajcani, J., D. Blaskovic, J. Svobodova, F. Ciampor, D. Huckova, and D. Stanekova. 1985. Pathogenesis of acute and persistent murine herpesvirus infection in mice. *Acta Virol.* **29**:51–60.
- Simas, J. P., and S. Efstathiou. 1998. Murine gammaherpesvirus 68: a model for the study of gammaherpesvirus pathogenesis. *Trends Microbiol.* **6**:276–282.
- Speck, S. H., and H. W. T. Virgin. 1999. Host and viral genetics of chronic infection: a mouse model of gamma-herpesvirus pathogenesis. *Curr. Opin. Microbiol.* **2**:403–409.
- Stevenson, P. G., and P. C. Doherty. 1999. Non-antigen-specific B-cell activation following murine gammaherpesvirus infection is CD4 independent in vitro but CD4 dependent in vivo. *J. Virol.* **73**:1075–1079.
- Stewart, J. P., E. J. Usherwood, A. Ross, H. Dyson, and T. Nash. 1998. Lung epithelial cells are a major site of murine gammaherpesvirus persistence. *J. Exp. Med.* **187**:1941–1951.
- Sunil-Chandra, N. P., S. Efstathiou, J. Arno, and A. A. Nash. 1992. Virological and pathological features of mice infected with murine gamma-herpesvirus 68. *J. Gen. Virol.* **73**:2347–2356.
- Sunil-Chandra, N. P., S. Efstathiou, and A. A. Nash. 1992. Murine gamma-herpesvirus 68 establishes a latent infection in mouse B lymphocytes in vivo. *J. Gen. Virol.* **73**:3275–3279.
- Thorley-Lawson, D. A. 2001. Epstein-Barr virus: exploiting the immune system. *Nat. Rev. Immunol.* **1**:75–82.
- Thorley-Lawson, D. A., and G. J. Babcock. 1999. A model for persistent

- infection with Epstein-Barr virus: the stealth virus of human B cells. *Life Sci.* **65**:1433–1453.
28. **Tibbetts, S. A., J. Loh, V. Van Berkel, J. S. McClellan, M. A. Jacoby, S. B. Kapadia, S. H. Speck, and H. W. T. Virgin.** 2003. Establishment and maintenance of gammaherpesvirus latency are independent of infective dose and route of infection. *J. Virol.* **77**:7696–7701.
  29. **Usherwood, E. J., A. J. Ross, D. J. Allen, and A. A. Nash.** 1996. Murine gammaherpesvirus-induced splenomegaly: a critical role for CD4 T cells. *J. Gen. Virol.* **77**:627–630.
  30. **Usherwood, E. J., J. P. Stewart, K. Robertson, D. J. Allen, and A. A. Nash.** 1996. Absence of splenic latency in murine gammaherpesvirus 68-infected B cell-deficient mice. *J. Gen. Virol.* **77**:2819–2825.
  31. **Virgin, H. W., and S. H. Speck.** 1999. Unraveling immunity to gamma-herpesviruses: a new model for understanding the role of immunity in chronic virus infection. *Curr. Opin. Immunol.* **11**:371–379.
  32. **Virgin, H. W. T., P. Latreille, P. Wamsley, K. Hallsworth, K. E. Weck, A. J. Dal Canto, and S. H. Speck.** 1997. Complete sequence and genomic analysis of murine gammaherpesvirus 68. *J. Virol.* **71**:5894–5904.
  33. **Virgin, H. W. T., R. M. Presti, X. Y. Li, C. Liu, and S. H. Speck.** 1999. Three distinct regions of the murine gammaherpesvirus 68 genome are transcriptionally active in latently infected mice. *J. Virol.* **73**:2321–2332.
  34. **Weck, K. E., M. L. Barkon, L. I. Yoo, S. H. Speck, and H. I. Virgin.** 1996. Mature B cells are required for acute splenic infection, but not for establishment of latency, by murine gammaherpesvirus 68. *J. Virol.* **70**:6775–6780.
  35. **Weck, K. E., S. S. Kim, H. I. Virgin, and S. H. Speck.** 1999. B cells regulate murine gammaherpesvirus 68 latency. *J. Virol.* **73**:4651–4661.
  36. **Weck, K. E., S. S. Kim, H. I. Virgin, and S. H. Speck.** 1999. Macrophages are the major reservoir of latent murine gammaherpesvirus 68 in peritoneal cells. *J. Virol.* **73**:3273–3283.
  37. **Willer, D. O., and S. H. Speck.** 2003. Long-term latent murine gammaherpesvirus 68 infection is preferentially found within the surface immunoglobulin D-negative subset of splenic B cells in vivo. *J. Virol.* **77**:8310–8321.